Journal of Luminescence 145 (2014) 65–70

Contents lists available at ScienceDirect

Journal of Luminescence

journal homepage: www.elsevier.com/locate/jlumin

Luminescence properties and energy transfer in $La_6Ba_4(SiO_4)_6F_2$:Ce^{3+},Tb^{3+} phosphors

Qingfeng Guo, Libing Liao*, Zhiguo Xia*

School of Materials Science and Technology, China University of Geosciences, Beijing 10083, China

ARTICLE INFO

Article history:
Received 20 January 2013
Received in revised form
19 May 2013
Accepted 10 July 2013
Available online 18 July 2013

Keywords:
Phosphors
Luminescence
Apatite
Hexagonal
Energy transfer

ABSTRACT

A series of new luminescent emission-tunable phosphors $La_6Ba_4(SiO_4)_6F_2$:Ce^{3+},Tb^{3+} with apatite structure have been synthesized by a high temperature solid-state reaction. X-ray diffraction, photoluminescence (PL) emission and excitation spectra, lifetime, as well as the effect of Tb^{3+} concentration were employed to characterize the resulting samples. The PL spectrum of $La_6Ba_4(SiO_4)_6F_2$:Ce^{3+},Tb^{3+} phosphor contains both the asymmetric broad-band blue emission (Ce^{3+} ion) and the line-type green emission (Tb^{3+} ion). The increased Tb^{3+} concentration induced the emitting colors to shift from blue to green region by the naked eye. Meanwhile, the energy transfer between Ce^{3+} and Tb^{3+} is thoroughly investigated, and the energy-transfer efficiency from Ce^{3+} to Tb^{3+} ion is also calculated. The results indicated that these phosphors could be considered as double emission phosphors for n-UV excited white light-emitting diodes.

1. Introduction

Recently, white light emitting diodes (w-LEDs) as lighting source have received significant attention due to their advantages, such as environmental friendliness, low cost, and good performance [1–4]. As we know, the w-LEDs based on YAG:Ce phosphors faced problems of high correlated color temperature and poor color rendition index (CRI). Alternatively, w-LEDs can be also fabricated by pumping tricolor phosphors coated on a near-UV (n-UV) LED chip, providing superior color uniformity, a high CRI value [5–8]. It is well-known that rare-earth (RE) ions play an irreplaceable role in lighting and display fields based on their 4f→4f or 5d→4f transitions [9,10]. In addition, energy transfer from sensitizer to activator by RE ions can induce interesting luminescence behaviors in many inorganic hosts [11–13]. Ce^{3+} ion is not only a well-known activator but also an important sensitizer for Tb^{3+} ions by transferring part of its excitation energy to Tb^{3+} [14–16]. Therefore, the luminescence originating from Ce^{3+}/Tb^{3+} couples can act as the green component for the n-UV LED.

Apatites act as the important inorganic mineral materials, which can be represented with the general formula $M_{10}(XO_4)_6Y_2$ ($M=Ca^{2+}$, Ba^{2+}, Ce^{3+}, La^{3+}, Y^{3+}, etc. and $X=P^{5+}$, As^{5+}, Si^{4+}, etc and $Y=OH^-$, F^-, Cl^-, etc.) [17,18]. Apatites compounds crystallize in the hexagonal system with space group $P6_3/m$, which have been widely used as host lattices for luminescent materials [19,20]. As is known to all, the $La_6Ba_4(SiO_4)_6F_2$ (LBSF) compound with apatite structure was firstly reported by Gong in 2005 [21]. This compound contains two cationic sites, that is, 9-fold coordinated 4f sites with C_3 point symmetry and 7-fold coordinated 6h sites with C_s point symmetry. Both sites can easily accommodate a great variety of RE^{3+} ions [22]. However, there are no reports about the detailed photoluminescence (PL) properties of Ce^{3+}, Tb^{3+}, and the sensitization effect of Ce^{3+}→Tb^{3+} luminescence in the LBSF host lattice. Accordingly, in this paper, we reported the synthesis of LBSF:Ce^{3+}/Tb^{3+} phosphors via the solid state reaction process, and a systematic study on the PL properties of these phosphors has been carried out in detail.

2. Experimental details

2.1. Synthesis

$BaCO_3$ (Aldrich, 99.9%), SiO_2 (Aldrich, 99.9%), NH_4HF_2 (Aldrich, 99.9%), La_2O_3 (Aldrich, 99.995%), CeO_2 (Aldrich, 99.995%), and Tb_4O_7 (Aldrich, 99.995%) were used as starting materials, which were mixed and ground according to the given stoichiometric ratio. Some excessive NH_4HF_2 (10%) is necessary for the loss of F source at high temperature. After all the materials were ground thoroughly in an agate mortar, the mixture was placed into an alumina crucible and was fired at 1400 °C for 4 h in a reducing atmosphere in flowing gas (5% H_2+95% N_2) with a flow rate of 0.5 L /min, and then the products were cooled to room temperature

---

* Corresponding authors. Tel.: +86 10 8232 2759.
E-mail addresses: lbliao@cugb.edu.cn (L. Liao), xiazg@cugb.edu.cn (Z. Xia).

0022-2313/$ - see front matter © 2013 Elsevier B.V. All rights reserved.
http://dx.doi.org/10.1016/j.jlumin.2013.07.035

naturally. Finally, the products were ground again into powder for measurement.

2.2. *Characterization*

Phase structures of the as-prepared samples were checked by X-ray powder diffractometer (D/max-rA 12 kw, Japan) with Cu Kα radiation ($\lambda = 1.5418$ Å) from 3° to 70° (2θ). The step scanning rate (2θ values ranging from 5° to 100°) used as Rietveld analysis was 3 s/step with a step size of 0.02°. Powder diffraction data were obtained using the computer software total Pattern Analysis System (TOPAS) package. The excitation and emission spectra of the samples were measured on a JOBIN YVON FluoroMax-3 fluorescence spectrophotometer with a photomultiplier tube operating at 400 V, and a 150 W Xe lamp used as the excitation lamp. The lifetimes were recorded on a spectro-fluorometer (HORIBA Jobin Yvon IBH Ltd., UK), and the 370 nm pulse laser radiation (370-nm Nano LED, model number 08254) was used as the excitation source. All the measurements were performed at room temperature.

3. Results and discussion

3.1. *XRD analysis*

Fig. 1 illustrates the XRD patterns of LBSF:0.05Ce^{3+} (a), LBSF: 0.05Ce^{3+},0.10Tb^{3+} (b), LBSF:0.05Ce^{3+},0.20Tb^{3+} (c), LBSF:0.05Ce^{3+}, 0.40 Tb^{3+} (d), and LBSF:0.05Tb^{3+} (e) samples annealed at 1400 °C for 4 h in H_2/N_2 (5%/95%). The standard data for LBSF (ICSD card no. 170852) is shown as a reference. It is found that the XRD patterns of all the samples are in good agreement with the reported LBSF phase (ICSD#170852) without any impurity phase. These results illuminate that doping of Ce^{3+} and Tb^{3+} does not cause any detectable change in LBSF, which indicates that the activator and co-activator have been incorporated in the host lattice. As suggested by Gong, LBSF belongs to the apatite-type compounds, which crystallizes in the hexagonal system with space group $P6_3/m$. The compounds contain two sets of nonequivalent crystallographic sites for cations, which are the 4f (C_3) site with nine-coordination [La^{3+}/Ba^{2+}(I)] and the 6h (C_s) site with seven-coordination [La^{3+}/Ba^{2+}(II)]. The occupancy of La^{3+} and Ba^{2+} in the 6h sites [La^{3+}/Ba^{2+}(I)] are about 75% and 25%, while the occupancy of La^{3+} and Ba^{2+} in the 4f sites [La^{3+}/Ba^{2+}(II)] are 37.5% and 62.5% respectively. The ratio of the La^{3+} site occupancies (La(I):La(II)) is 3.00 [21]. On the basis of the effective ionic radii and charge balance, we suggest that Ce^{3+}/Tb^{3+} ions prefer to occupy La^{3+}. Because the ionic radius of coordinated Ce^{3+}/Tb^{3+} ions are similar to La^{3+} in either seven- or nine-fold coordination, the 4f site with nine-coordination [La^{3+} (I)] and the 6h site with seven-coordination [La^{3+} (II)] were randomly occupied by Ce^{3+} or Tb^{3+}. In addition, the structure parameters and ionic radii of given coordination numbers (CNs) are shown in Table 1 [23].

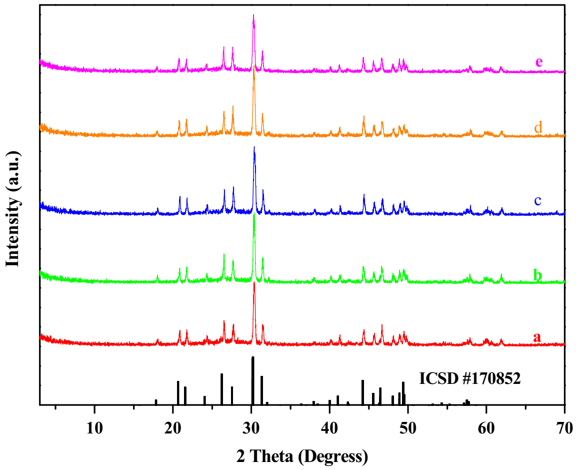

Fig. 1. X-ray diffraction patterns of $La_6Ba_4(SiO_4)_6F_2$:0.05Ce^{3+} (a), $La_6Ba_4(SiO_4)_6F_2$: 0.05Ce^{3+},0.10Tb^{3+} (b), $La_6Ba_4(SiO_4)_6F_2$:0.05Ce^{3+},0.20Tb^{3+} (c), $La_6Ba_4(SiO_4)_6F_2$:0.05Ce^{3+}, 0.40Tb^{3+} (d), and $La_6Ba_4(SiO_4)_6F_2$:0.05Tb^{3+} (e) samples annealed at 1400 °C for 4 h in H_2/N_2 (5%/95%). The standard data for LBSF (ICSD card no. 170852) is shown as a reference.

The experimental and simulated XRD patterns of $La_{5.95}Ce_{0.05}Ba_4(SiO_4)_6F_2$ and $La_{5.6}Tb_{0.4}Ba_4(SiO_4)_6F_2$ compounds are shown in Figs. 2 and 3. Solid red lines are calculated intensities, and circles are the observed intensities, and black solid lines for the difference between the observed and the calculated intensities. Short vertical lines below the profiles show the position of Bragg reflections of the calculated pattern. Both compounds were indexed on the hexagonal system with the space group of $P6_3/m$. After converging the reliability factors R_p and R_{wp} to 9.21% and 12.52%, respectively, the lattice constants of $La_{5.95}Ce_{0.05}Ba_4(SiO_4)_6F_2$ were revealed and listed in Table 2. As is shown in Table 3, the structure of $La_{5.6}Tb_{0.4}Ba_4(SiO_4)_6F_2$ refined finally converged to $R_{wp} = 10.84\%$, and $R_p = 7.82\%$. There are two different La sites in LBF. La (I) is the 9-fold coordinated 4f sites with C_3 point symmetry and La (II) is the 7-fold coordinated 6h sites with C_s point symmetry. According to the results shown in Table 2 and Table 3, Ce^{3+} and Tb^{3+} ions entered both the two different types of La sites with seven- or

Table 1
Structure parameters of LBSF and ionic radii (Å) for given CNs of Ba^{2+}, Ce^{3+}, Tb^{3+}, and La^{3+}, ions.

Ion	Sites	Symmetry	Ionic radius (Å) CN=9	Ionic radius (Å) CN=7
La^{3+}	4f/6h	C_3/C_s	1.216	1.10
Ba^{2+}			1.470	1.38
Ce^{3+}			1.196	1.07
Tb^{3+}			1.095	0.98

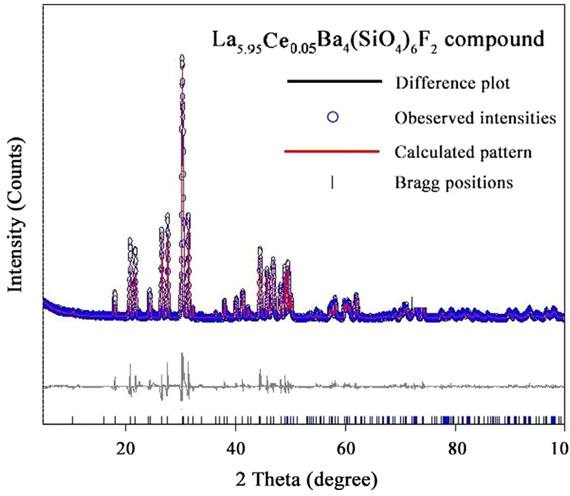

Fig. 2. Rietveld analysis patterns for X-ray powder diffraction data of $La_{5.95}Ce_{0.05}Ba_4(SiO_4)_6F_2$ compound. Solid red lines are calculated intensities, and circles are the observed intensities. Black solid lines for the difference between the observed and the calculated intensities. Short vertical lines below the profiles stand show the position of Bragg reflections of the calculated pattern. (For interpretation of the references to color in this figure legend, the reader is referred to the web version of this article.)